Journal of Geography, Environment and Earth Science International

Volume 28, Issue 5, Page 1-15, 2024; Article no.JGEESI.115647
ISSN: 2454-7352

Application of Airborne Magnetic Data to Assess the Structures that Favour Gold Mineralization within Southern Parts of Katsina State, Nigeria

Akpaneno, A. F. [a*] and Tawey, M. D [b]

[a] Department of Geophysics, Federal University Dutsinma, Katsina State, Nigeria.
[b] Groundwater Department, National Water Resources Institute, Mando Road, Kaduna, Nigeria.

Authors' contributions

This work was carried out in collaboration between both authors. Both authors read and approved the final manuscript.

Article Information

DOI: 10.9734/JGEESI/2024/v28i5766

Open Peer Review History:
This journal follows the Advanced Open Peer Review policy. Identity of the Reviewers, Editor(s) and additional Reviewers, peer review comments, different versions of the manuscript, comments of the editors, etc are available here: https://www.sdiarticle5.com/review-history/115647

Original Research Article

Received: 05/02/2024
Accepted: 09/04/2024
Published: 12/04/2024

ABSTRACT

The Nigerian schist belts are endowed with gold mineralisation and to delineate the geological structures that favour gold mineralisation, the airborne magnetic data that cover the study area was employed. Also, the residual magnetic anomaly data of the research area was reduced to the Equator (RTE) followed by the application of the centre for exploration targeting (CET) plug-in and three source edge mapping techniques; analytic signal (AS), first vertical derivative (FVD) and the horizontal gradient magnitude (HGM), for structural delineation and subsequently the structural density map of the area was produced. Structural density varies from 0.186 km/km2 low to 0.93 km/km2 high. Portions within the study area with high structural densities are Bakori in the southwest, Shanono in the northeast, Gwarzo situated directly south of Shanono, north and south of Karaye, the border between Kafur and Rogo in the south, all within the schist. Since structures

**Corresponding author: E-mail: aniefiokakpaneno@gmail.com;*

are conduits for the migration of mineralisation fluids, areas with high structural densities will be viable for gold mineralisation. Also, comparing the structural density map of the area to the analytic signal map of the area has revealed the high structural density portions to coincide with the high analytic signal zones. This implies that structures within these portions are responsible for the migration of mineralization fluid into these environments.

Keywords: Gold mineralization; structural densities; CET; HGM; FVD; AS.

1. INTRODUCTION

The Nigeria landmass hosts several solid minerals [1,2,3], particularly gold, which are widely distributed across the western half of the country where the present study area is situated (schist belts), (Fig. 1). The mining of these solid minerals especially gold in Nigeria, is regarded as a driving force for the growth of the country's economy [4]. Deposits of gold and other mineral inclusions have been reported within the schist belts of the country [5,6,1,2]. Within the Nigerian schist belts, most mineralized zones are structurally controlled and are associated with shear zones and hydrothermal veins formed in response to the tectonic stress field [7,8,9,10].

Geological structures such as fractures, faults, folds, and joints play a very important role in gold mineralization as conduits for the mineralization solution and foci points of emplacement of mineralization fluid [4]. Thus, faults and shear zones are potential pathways of hydrothermal fluids [9,11,12] and thus, understanding the

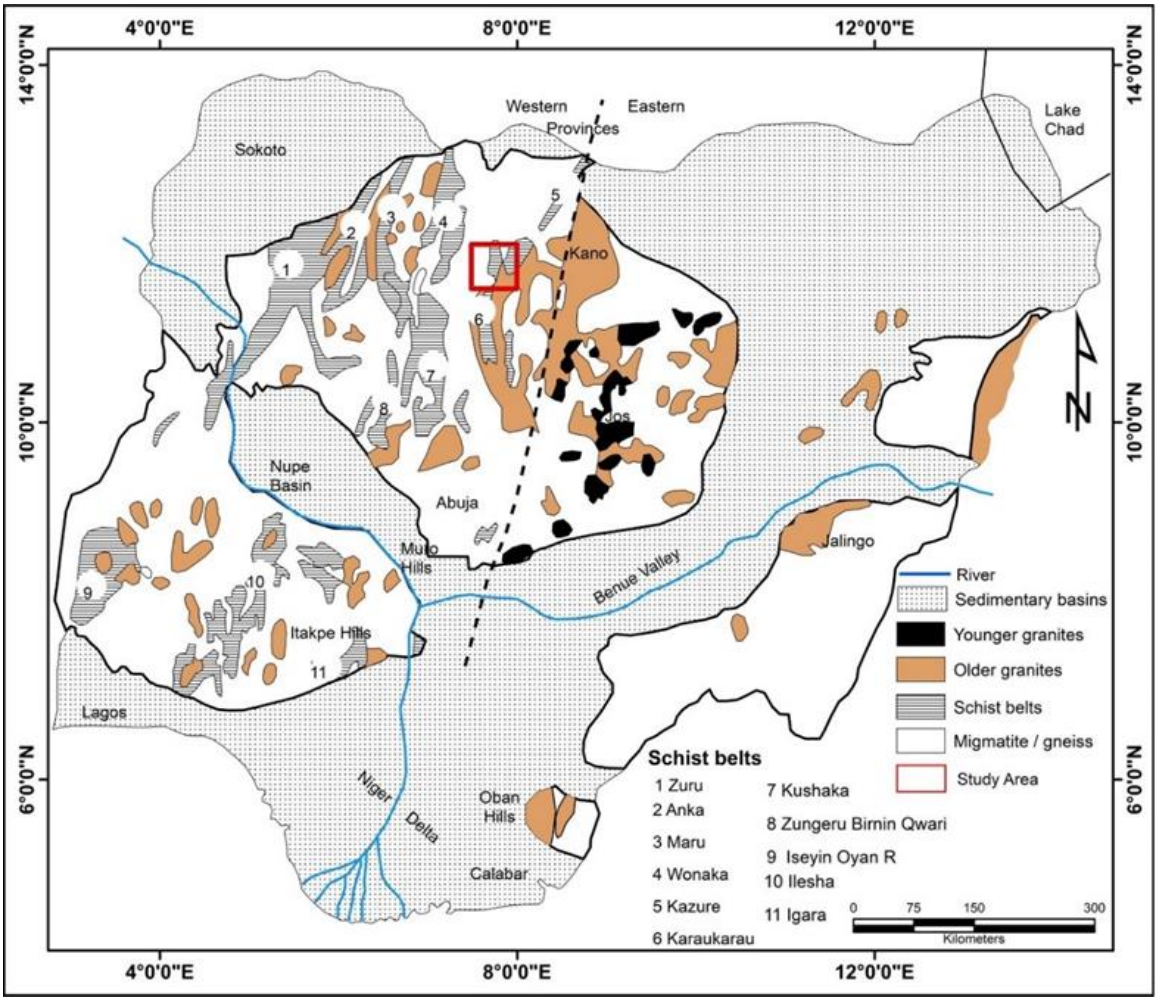

Fig. 1. Map showing the study area with the Nigerian schist belts Modified from [11]

structural framework of a mineralized area, the distribution and orientation of the structures, (joint, fault, fractures, and shear zones), their formation during the structural evolution and the tectonic conditions are key to understanding the formation, origin and location of mineral deposits [13]. These structures are often concealed beneath the surface and in some cases, they are deeply seated as such require a geophysical approach that can delineate these subtle structures that may be responsible for the migration of hydrothermal fluid relevant and responsible for the deposition of Gold [14].

The use of airborne magnetic data has provided a quick, economical, and regional-scale prospecting possibility as a flexible geophysical method for mapping surface and subsurface features and geology structures based on the variation of the geomagnetic field [15,16,17]. The airborne magnetic approach has been used to locate fractures, faults, and ring systems in basement rocks, which may influence mineralization [18,9,19,20,21,22], and have been used to map geologic structures related to orogenic gold deposit [23,24,25]. Its application in mineral exploration, especially around hydrothermal alteration prospects, is to accentuate the structural regime in the region to define suitable pathways that may have supported hydrothermal fluid circulation systems relevant to mineral accumulation [26,27].

In keeping with their relevance, geophysical investigations of the physical properties of geologic bodies (e.g. size, body geometry, depth, density contrast, and susceptibility contrast) provide supplementary and superior regional correlation to information gained from geology [20]. This geophysical technique improves our understanding of the structural properties found on a regional scale. It also helps geological mapping in identifying areas of sedimentary, metamorphic, and intrusive rock growth, as well as zones of tectonic deformation. Geophysical investigations of this type have been extremely important in revealing a more precise and better knowledge of the distribution and evolution of geologic provinces [28]. These approaches aid in identifying boundaries and the true extent of significant structural units that were difficult to properly find using geologic mapping [29].

Several research works have been published within the Nigerian basement complex mostly in the schist belts for structures, hydrothermal alteration zones delineation for gold employing either only the magnetic method or the integration of magnetic with radiometric or the remote sensing data [5], [18,9,19,30,21,32,10,6,23,33,34,35,36,37]. Since these methods are essential in characterizing geological features including faults, folds, shear zones, and other favourable places for mineralization, they are widely used globally as fundamental tools for geological interpretations [14,38,39,40].

1.1 Location and Topography of the Study Area

The study area is located within the northwest part of Nigeria, particularly the schist belt (Fig. 1), and is bordered by Latitude 110 301 N to Latitude 120 N and Longitude 70 301 E to Longitude 80 E (Fig. 2). It is situated between Katsina and Kano states (Fig. 2) and extend from the north of Kurba in the west through north of Dan Tatashi to Northeast of Gwarzo in the east. It also extends from southwest of Tamarke in the southwest to the south of.

Barbaji in the southeast with topography that varies from 5199 m low to 618 m high (Fig. 3). Low elevated portions above sea level are observed in the east around Zoza, Mafuta, Kwari, west of Masari, South of Kunnuwa, Dakanjiba, and south of Gwarzo. Areas with high topography above the sea level are Tamarke in the southwest, Tsiga, Mararaban Kankaro, Malumfashi, Kurri and Dan Tatashi.

The aim of this research is to delineate the magnetic structures that favour gold mineralisation within the study area and the objectives are to

i. Use three source edge mapping techniques first vertical derivative (FVD) provided by [41], analytic signal (AS) put forward by Nabighian, 1984 and the horizontal gradient magnitude (HGM) by [42], to map the structures within this area and comparatively discuss the structures delineated by these three methods.

ii. Delineate areas with high structural density that may favour gold mineralisation.

iii. Carry out statistical trend analysis of the delineated structures to understand the structural regime that has affected the study area.

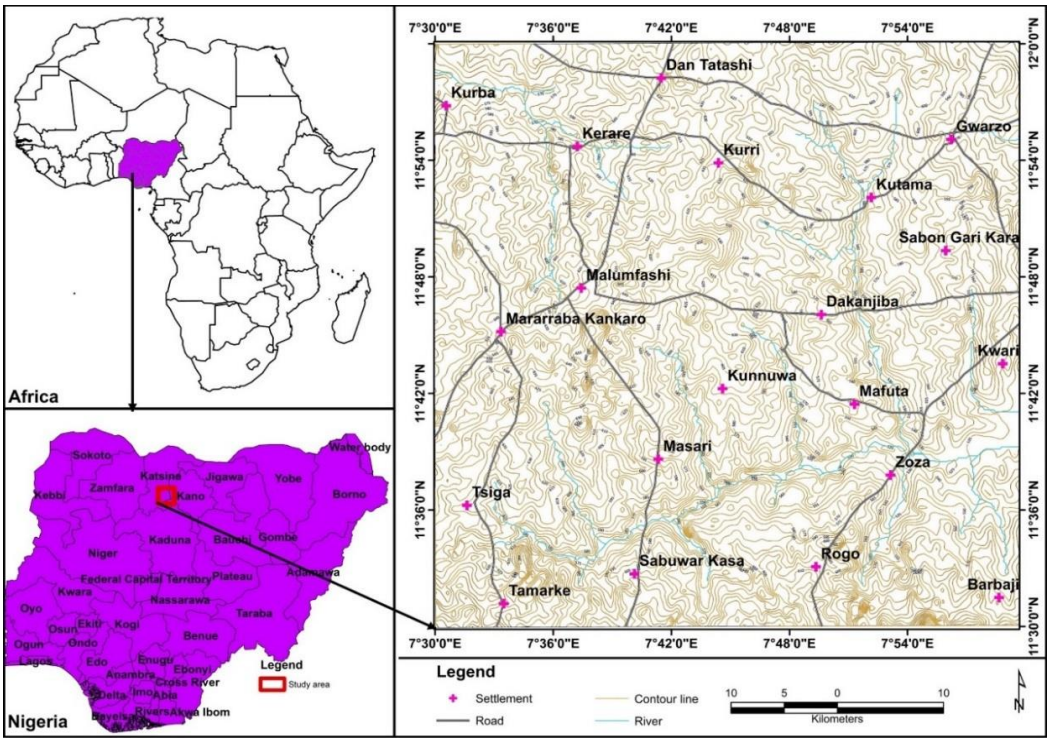

Fig. 2. Location of the study area

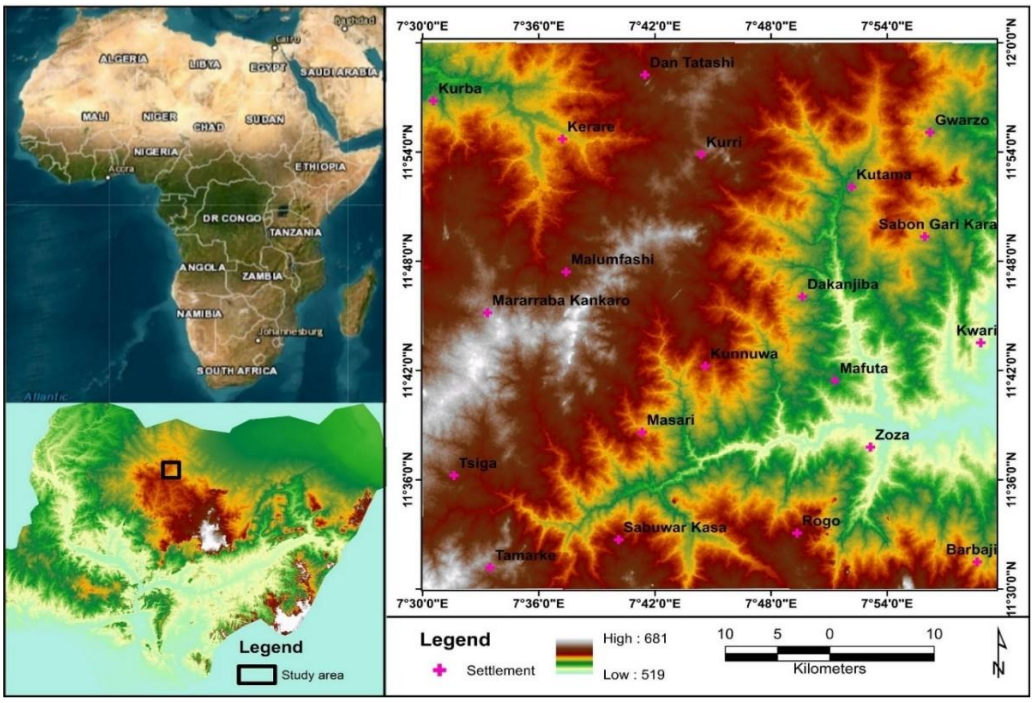

Fig. 3. Digital elevation model showing topographical variation across the area.

1.2 Tectonic Settings and Geology

The Schist Belts are low-grade, mostly metasediments that trend from north to south and occupy Nigeria's western region (Fig. 1), also situated within the Nigerian basement complex and part of an axis called the Togo-Benin-Nigeria swell (Fig. 4a), [43]. Tectonically, the area is situated within the Pan-African mobile belt (Fig. 4a), and adjacent to the west of the

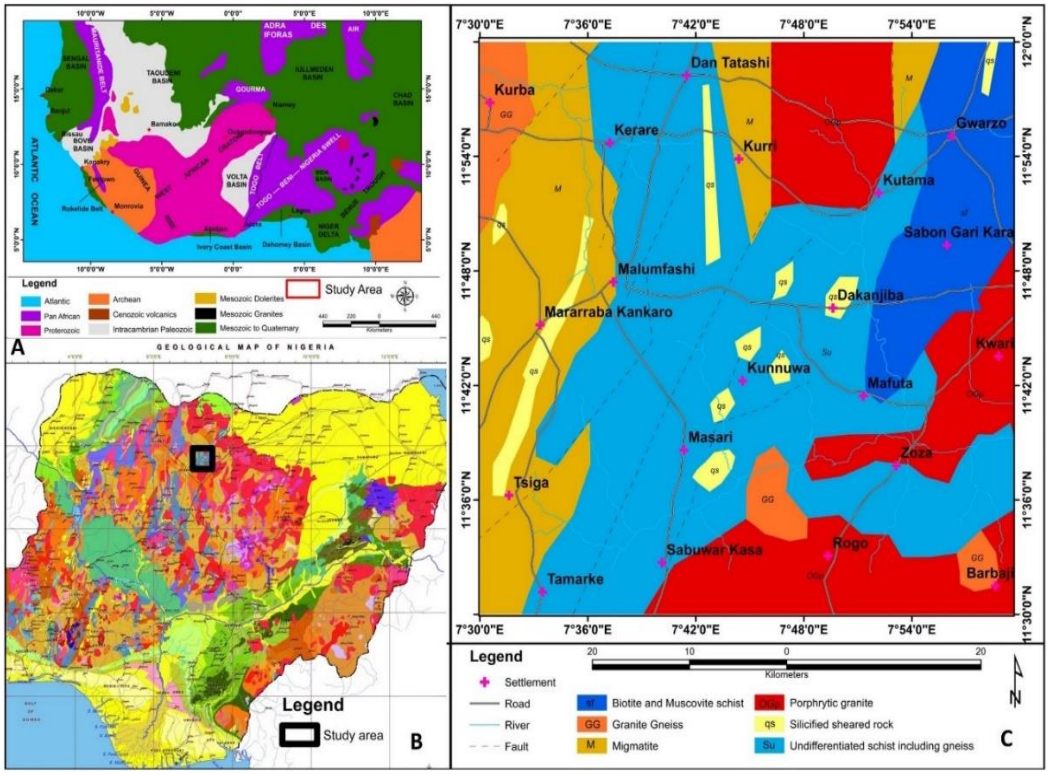

Fig. 4a. Generalized geologic map of West Africa b. Geologic map of Nigeria and c. geologic map of the study area Modified from [2], and [43]

swell is the Togo belt that borders the Volta Basin. The north of the swell is the Iullemeden Basin and to the east of it is the Chad Basin [43]. In age, rock within the schist belts is Upper Proterozoic and has been infolded into the migmatite-gneiss-quartzite complex. The lithological composition of rocks within the schist belts includes fine- grained clastics, pelitic schists, Phyllites, banded iron formation, marbles / dolomitic marbles and Amphibolites. [44] has suggested several basins of deposition for schist belts while McCurry [45] envisages the schist belts as relicts of a single supracrustal cover.

[46] See the schist belts to be fault-controlled rift-like structures [47] and other researchers, based on structural and lithological associations, suggest that there are different ages of the sediments. However, [48] disagree with this conclusion and show that both series contained identical deformational histories. The structural relationships between the schist belts and the basement were considered by [49] to be conformable metamorphic fronts and it was [48] who first mapped a structural break. The schist belts have been mapped and studied in detail in the following localities: Maru, Anka, Zuru, Kazaure, Kusheriki, Zungeru, Kushaka, Isheyin Oyan, Iwo, and Ilesha where they are known to be generally associated with gold mineralization.

2. MATERIALS AND METHODS

The data used for this research was acquired from the Nigerian Geological Survey Agency (NGGSA), Abuja. The project was a collaboration between the World Bank and the Nigerian government that spanned two phases. Phase one was sponsored solely by the Nigerian government while phase two was a joint funding between the World Bank and the Nigerian government. Fugro Airborne Surveys was responsible for the collection and interpretation of the raw data collected. The airborne geophysical survey was done by the Fugro Airborne surveys on behalf of the Nigerian Geological Survey Agency (NGSA) at an interval of 0.1 seconds (about 7.5 meters), the data were recorded for magnetic measurements. With a flight line spacing of five hundred (500) meters, a terrain clearance of 80 meters, and a tie line spacing of 2000 meters in the NE-SW direction, the airborne survey was flown perpendicular to the major geological trends in the area in the NW-SE direction.

2.1 Processing of Magnetic Data

The shape of magnetic anomaly at low latitudes just like the present study area is said to be distorted or skewed as a result of its declination and inclination angles. To overcome this unwanted distortion in the shapes, sizes, and locations of magnetic anomalies, due to the effect of inclination and declination of the Earth's magnetic Feld, the reduced-to-equator (RTE) approach was applied to produce a magnetic map comparable to what would have been acquired if the area had been surveyed at the magnetic equator, under the premise that all magnetic fields visible in the research region are the consequence of induced magnetic effects. The fast Fourier transformation (FFT) was applied to RTE aeromagnetic data to produce regional and residual magnetic component maps. The first vertical derivative (FVD), and horizontal gradient magnitude (HGM) methods were also applied on the RTE airborne magnetic map of the study area to detect the structures that may play a key role in mineral exploration within this part of Katsina state in the same vein, the analytic signal amplitude was applied to the TMI data also for source location and structural delineation.

To delineate the structures (source edges) within the study area, the Centre for Exploration Targeting (CET) method was applied to the RTE data. The CET is an algorithm suite that enhances, detects lineaments and analyses complex structures in potential field data [50]. It automatically delineates lineaments and identifies promising areas of ore deposits using total magnetic intensity data, highlighting junction points and high lineament densities for further exploration. It identifies texture zones in a restricted magnetic response, often owing to rock edges, elongated structures, and intrusions [51]. These zones are expressed as skeletal structures, with output data showing deviations and offsets within the structural characteristics [52]. The CET technique was also applied to the FVD, AS and HGM map data where the structures were subsequently mapped out. The roses diagrams of the delineated structures were plotted for trends and the structural density map of the RTE structural map was produced to ascertain the most probable portions for Gold mineralisations.

- The analytic signal amplitude (A) of a potential field anomaly as defined by the orthogonal gradient of the total magnetic field using the expression, Equation 1:

$$|A(X,Y)| = \sqrt{\left(\frac{\delta T}{\delta x}\right)^2 + \left(\frac{\delta T}{\delta y}\right)^2 + \left(\frac{\delta T}{\delta z}\right)^2} \quad (1)$$

where A(x, y) is the amplitude of the analytic signal at (x, y) and is the observed magnetic anomaly at (x, y), by [53].

- The first vertical derivative provided by [41] is given by Equation 2:

$$M(x,y) = M(x,y)\sqrt{\left(\frac{x^2+y^2}{n}\right)^n} \quad (2)$$

with n being the order of the derivative.

- The horizontal gradient magnitude is given by [42], for the magnetic field is given as Equation 3:

$$HGM(x,y) = \sqrt{\left(\frac{\partial M}{\partial x}\right)^2 + \left(\frac{\partial M}{\partial y}\right)^2} \quad (3)$$

where and are the horizontal derivatives of the magnetic field in the two directions and respectively.

3. RESULTS AND DISCUSSION

Fig. 5a represents the RTE map, Fig. 5b represents the AS map, Fig. 5c represents the FVD map and Fig. 5d represents the HGM map of the study area and these maps are briefly explained below.

3.1 The RTE Map

The RTE map represents the residual magnetic intensity reduced to the equator map of the study area overlayed with the local government shapefile in white colour. Because the study area is situated near the equator, the anomaly map is represented by low positive anomaly values. Magnetic anomaly values range from -105.3nT low to 69.6 nT high. Low values areobserved around Gwarzo in the northeast toward the north of Shanono. Other low values are observed around Kafur, south of Karaye, north to the east of Kafur and south of Bakori in the southwest. Areas observed with high magnetic anomaly are portions around the North of Karaye, Rogo, and Kiru, the boundary between Gwarzo and Shanono which could be structures, and Malumfashi to Musawa across the north of the study area. Anomaly trends are generally irregular. There is an observed northeast-to-southwest magnetic low trend that represents structure passing through Bakori in the

southwest through the centre of the study area to the northeast (Fig. 5a).

3.2 AS Map

The AS image (Fig. 5b) highlights the variation in the distribution of magnetic sources in the study area. Discontinuities (structures) and anomaly texture are also accentuated. The AS map displayed high amplitudes from the northwest of the map and stretched to the southern end of it and there are also isolated occurrences of high intensity around the southwest and north-western part of the study area. The AS amplitude maximises over the edge of the magnetic structures as a result, the high magnetic anomalies zones are associated with highly rich ferromagnesian-bearing rocks with minor felsic minerals [54].

The study area could also be said to have exhibited three different magnetic zones in this area of study based on the amplitude of the anomalies within this area. Low magnetic zone with an amplitude less than 0.1nT/m, moderate magnetic zone (MM) with an amplitude of 0.1 m to 0.2 nT/m and the areas with high magnetic anomaly zones having amplitudes above 0.2 nT/m.

3.3 FVD Map

The first vertical derivative filter enhanced the high frequency (short wavelength) part of the data, which allows small and large amplitude responses to be more equally represented to observe near-surface source magnetic features that are associated with geological structures in the study area. The colour image of the first vertical derivative of the study area (Fig. 5c) enhanced the image by showing major structural and lithological detail which was not obvious in the magnetic residual map.

In Fig. 5c, the map revealed high frequency (short wavelength) signatures (anomalies) with clear edges along the northwestern part of it to the south. These short-wavelength signatures are also observed at the southwestern part of the map with the NE-SW trend. Structural trends generally on the map are NE-SW and NW-SE tectonic trends as revealed by the FVD map.

3.4 HGM Map

The horizontal gradient approach has been applied in this study because it has the biggest benefit in that it is least affected by data noise; it just involves the computation of the field's two first-order horizontal derivatives and the horizontal gradient filter, which may be calculated by [55].

HGM and AS both peak over the source edges, but the form of the analytic signal is unaffected by magnetization direction or local magnetic field. The HGM map exposes more structural complexity, including lithological connections of multiple geological entities, than the AS map, and contacts formed in HGM maps, according to [55], are expected to be dislocated in the down-dip direction for dipping contact sources. Fig. 5d depicts the locations of HGM maxima, and the map reveals that the maxima are generally in the NE-SW and NW-SE directions, with the NE-SW trends predominating.

3.5 Structural Analysis

Structures (Lineaments) were analysed to extract further information on the distribution and nature of the lineaments and for this purpose, a conventional technique called rose diagram was applied. A Rose diagram was used to display graphically different tendencies for structures like joints or fault planes representing the angular relationships of the geologic map data. The purpose of this study is to analyse the spatial distribution of lineaments extracted from aeromagnetic images according to their length and orientation to contribute to the understanding of the faults of the study area. Fig. 6 represents the magnetic structures delineated from a. FVD map, b. AS map, c. HGM map and d. RTE map using CET. From the maps, the structural trend most predominant and common to the AS, FVD, and HGM methods is the NE-SW trend (Pan-African), as revealed from the rose's diagrams (Figs. 7 a, b, and c). Thus, this revealed the tectonic regime and episode that have affected the study area and its surroundings. The second tectonic event within the Pan African event is revealed in the CET structural map delineated using the RTE map (WNW-ESE), as revealed in the RTE roses diagram (Fig. 7d).

3.6 Structural Density map

Fractures, faults, folds, and joints are essential geological features in gold mineralization because they operate as conduits for the mineralization solution and focal areas for mineralization fluid emplacement [10]. Thus, faults and shear zones are potential pathways of

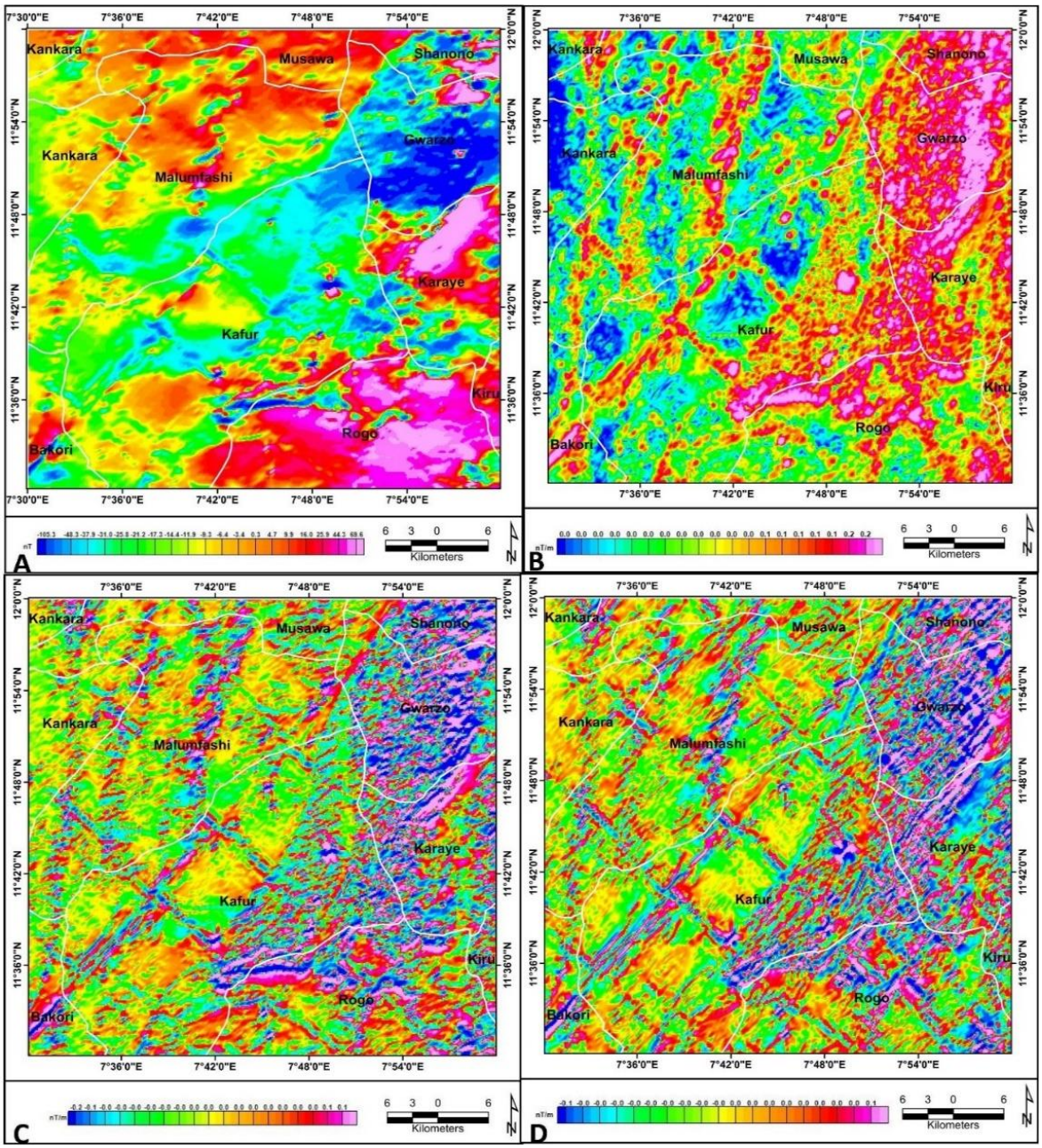

Fig. 5a. RTE map b. AS map c. FVD map and d. HGM map

hydrothermal fluids [9,11,12]. Within the Nigerian schist belts, most mineralized zones are structurally controlled and are associated with shear zones and hydrothermal veins formed in response to the tectonic stress field [7,4,9], portions with high structural density will have high prospect for gold mineralisation within this area. Fig. 8 represents a structural density map of the study area and from the map, areas with a high structural density that will favour gold occurrence are observed around Shanono, Gwarzo, Karaye, North and west of Rogo and west of Kafur.

Comparing the structural density map of the area to the analytic signal map of the area has revealed the high structural density portions to coincide with the high analytic signal zones (Figs. 9 a and b). This implies that structures within these portions are responsible for the migration of mineralisation fluid into these environments.

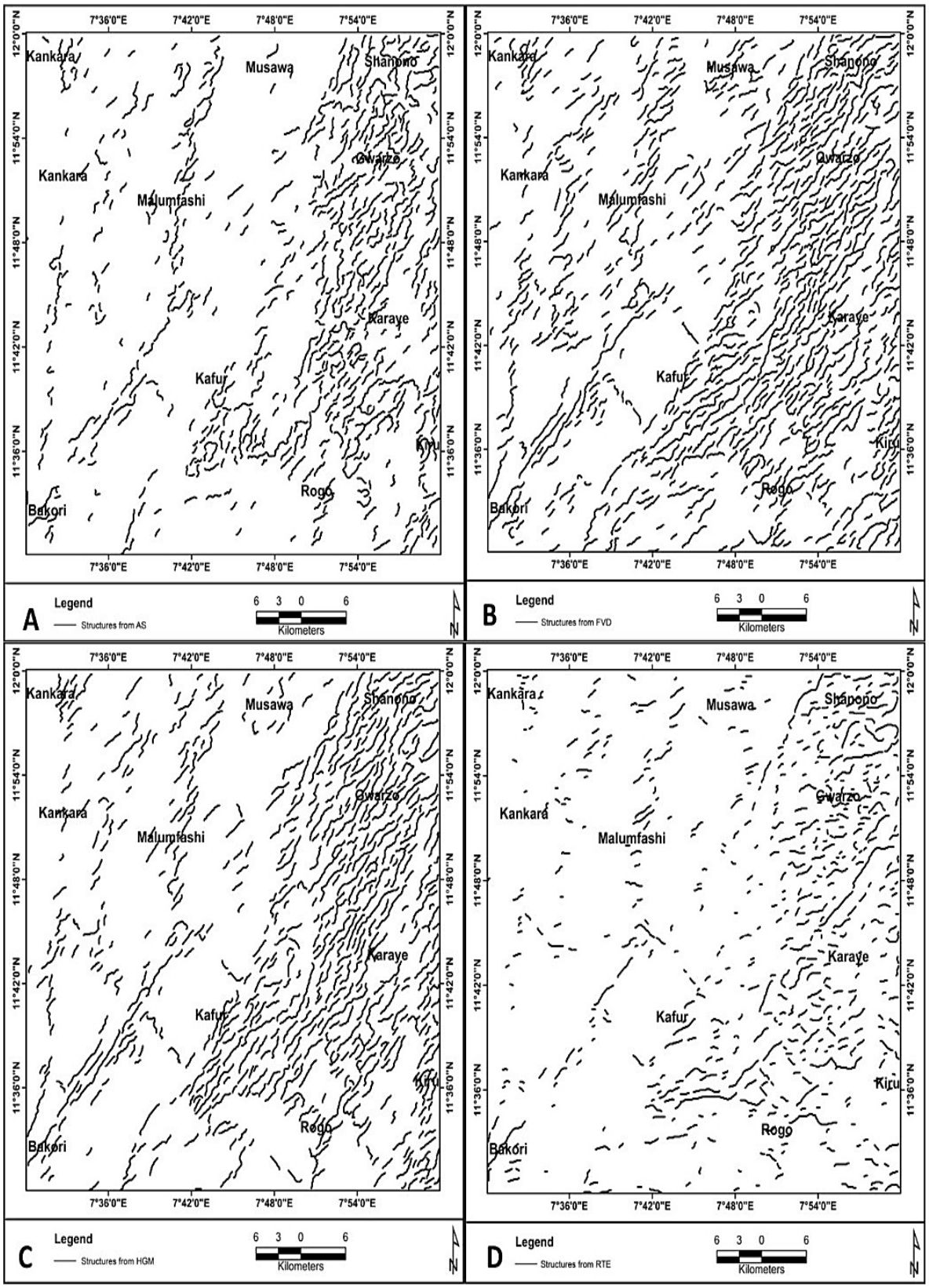

Fig. 6a. AS structures b. FVD structures c. HGM structures and d. CET structures from RTE

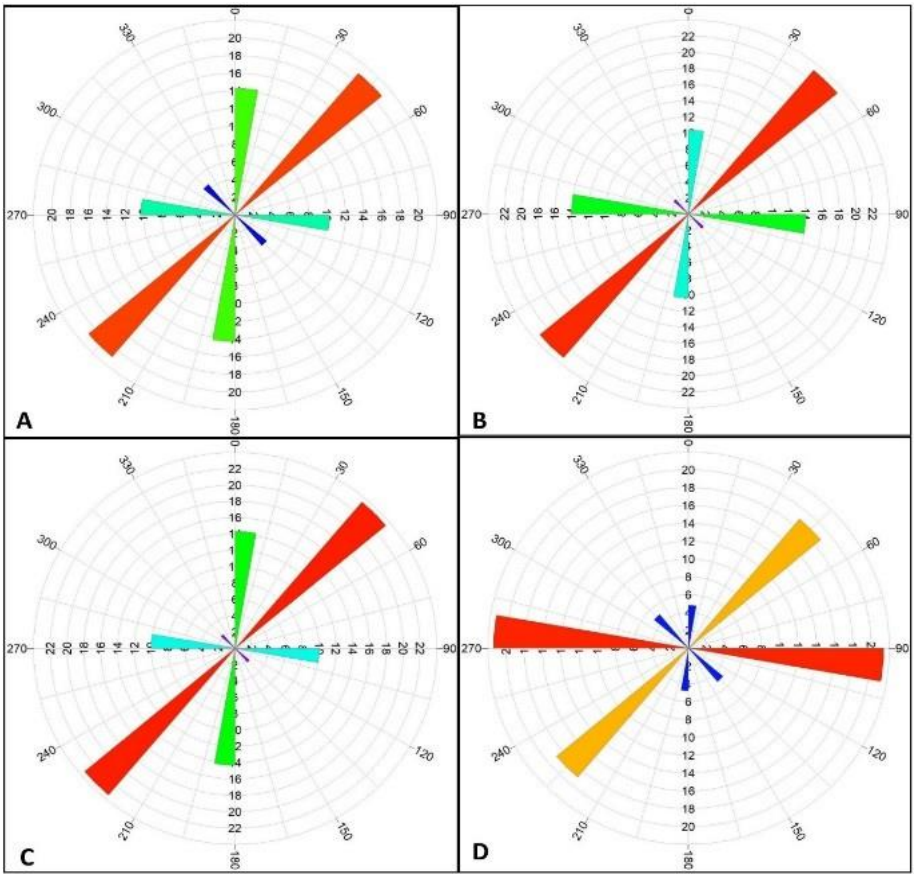

Fig. 7. Roses diagram. a. AS structures b. FVD structures c. HGM structures and d. CET structures from RTE

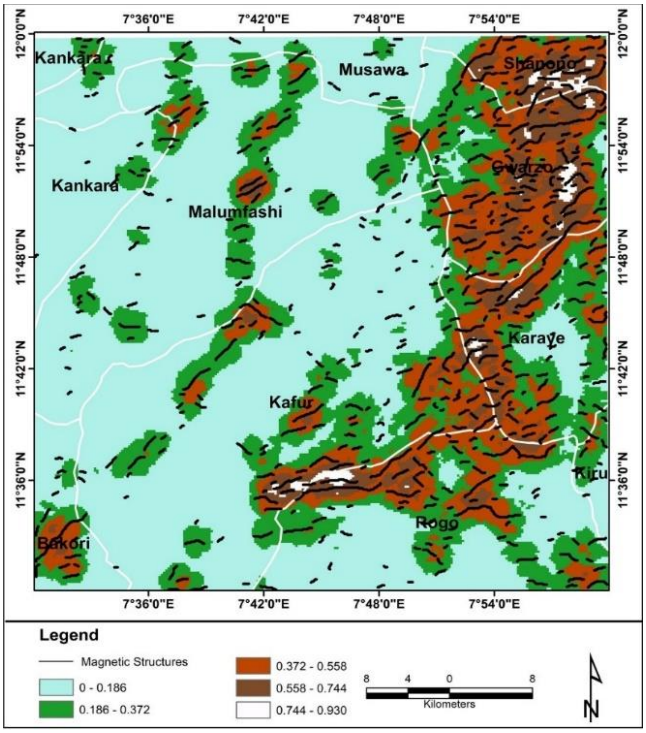

Fig. 8. Structural density map of the study area

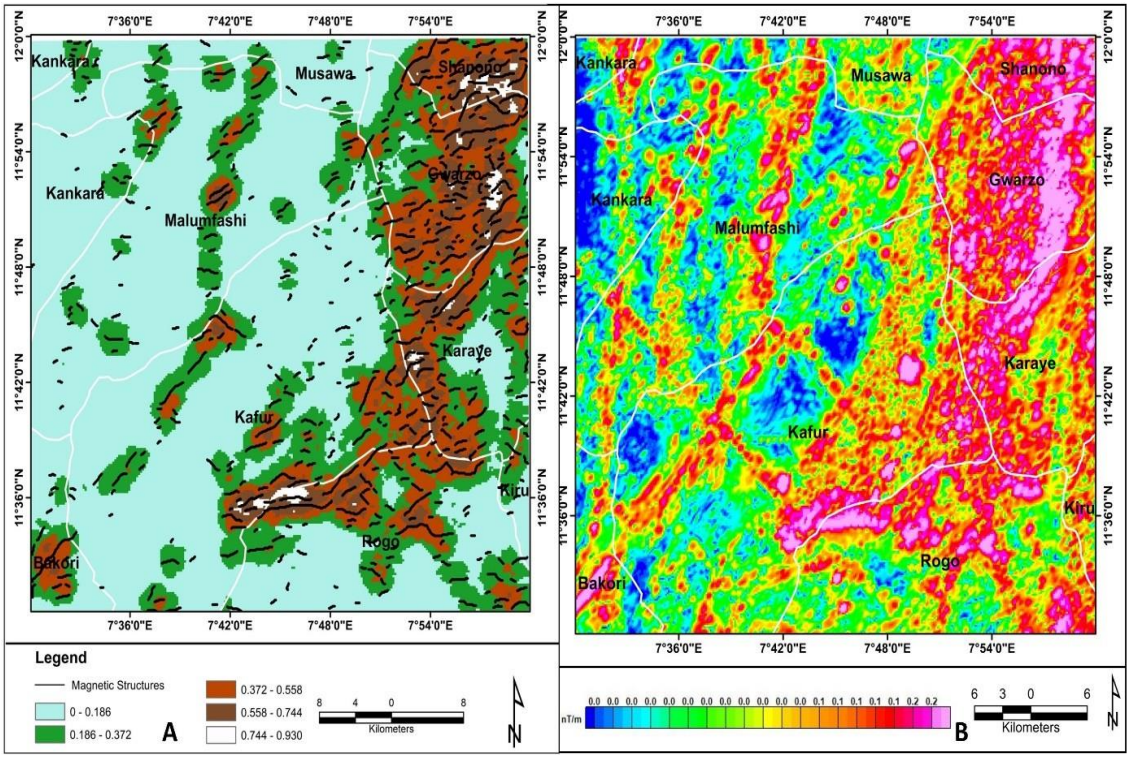

Fig. 9a. Structural density map of the study area b. analytic signal map of the area

4. CONCLUSION

The study area's RTE map shows residual magnetic intensity reduced to the equator map, with low positive anomaly values. Low values are found around Gwarzo, Kafur, Karaye, and Bakori. High anomaly areas include Karaye, Rogo, Kiru, and Malumfashi to Musawa. Anomaly trends are irregular, with a northeast-to-southwest magnetic low trend indicating structure passing through Bakori.

The AS map reveals magnetic source distribution variations in the study area, with high amplitudes from the northwest to the southern end and isolated high-intensity zones around the southwest and north-western parts. The study area generally exhibited three magnetic zones: low, moderate, and high zones, with amplitudes ranging from 0.1 nT/m to 0.2 nT/m, respectively.

The first vertical derivative filter improved data representation by enhancing high frequency, allowing equal representation of small and large amplitude responses, and enhancing colour images, revealing structural and lithological detail. The map reveals high-frequency anomalies along the northwestern and southwestern parts of the map, with structural trends primarily in the NE-SW and NW-SE direction which represent tectonic trends within the area.

The HGM maps reveal structural complexity and dislocated contacts, with NE-SW trends dominating.

The structural trend most predominant and common to the AS, FVD, and HGM methods is the NE-SW (Pan-African) trend, as revealed from the rose's diagrams. Thus, this revealed the tectonic regime and episode that have affected the study area and its surroundings. The second tectonic event within the study area is revealed in the CET structural map delineated using the RTE map (WNW-ESE), as revealed in the RTE roses diagram. From the structural density map of the area, areas with a high structural density that will favour gold occurrence are observed around Shanono, Gwarzo, and Karaye, North and west of Rogo and west of Kafur. Comparing the structural density map of the area to the analytic signal map of the area has revealed the high structural density portions to coincide with the high analytic signal zones This implies that structures within these portions are responsible for the migration of mineralisation fluid into these environments.

COMPETING INTERESTS

Authors have declared that no competing interests exist.

REFERENCES

1. Obaje NG. Geology and resources of Nigeria 120 lectures notes in Earth Sciences. Springer-Verlag; 2009. Available:https://doi.org/ 10.1007/978-3-540-92685-6
2. Nigeria Geological Survey Agency (NGSA). Mineral resources map of Nigeria (2006 Ed.). Published by the Authority of the Federal Republic of Nigeria. 2006;1.
3. Nigeria Geological Survey Agency (NGSA) Geological map of Nigeria (2009 Ed.). Published by the Authority of the Federal Republic of Nigeria. 2009;1.
4. Augie AI, Salako KA, Rafiu AA, Jimoh MO. Geophysical assessment for gold mineralization potential over the southern part of Kebbi State using aeromagnetic data. Geology, Geophysics and Environment. 2022a;48(2):177-193.
5. Akinlalu AA. Radiometric mapping for the identification of hydrothermally altered zones related to gold mineralization in Ife–Ilesa schist belt, southwestern Nigeria. Indonesian Journal of Earth Sciences. 2023;3(1):51.
6. Augie AI, Sani AA. Interpretation of aeromagnetic data for gold mineralisation potential over Kabo and its environs NW Nigeria. Savanna J Basic Appl Sci 2020;2(2):116–23.
7. Ajakaiye DE, Hall DH, Ashiekaa JA, Udensi EE Magnetic anomalies in the Nigerian continental mass based on aeromagnetic surveys. Tectonophysics. 1991;192(1):211-230.
8. Kearey P, Brooks M, Hill I. An introduction to geophysical exploration. Blackwell Scientific Publications, New York; 2002.
9. Tawey MD, Adetona AA, Alhassan UD, Rafiu AA, Salako KA, Udensi EE. Aeroradiometric data assessment of hydrothermal alteration zones in parts of north central Nigeria. Asian Journal of Geological Research. 2021;4(2):1-16.
10. Augie AI, Salako KA, Rafiu AA, Jimoh MO. Geophysical magnetic data analyses of the geological structures with mineralization potentials over the southern part of Kebbi, NW Nigeria. Mining Science. 2022b; 29;179-203.
11. Tawey MD, Adetona AA, Alhassan DU, Salako KA, Rafiu AA, Udensi EE. Edge Detection and Depth to Magnetic Source Estimation in Part of Central Nigeria Physical Science International Journal. 2020b;24(7):54-67. Article no. PSIJ.60263 ISSN: 2348-0130.
    DOI: 10.9734/PSIJ/2020/v24i730203
12. Sani AA, Augie AI, Aku MO. Analysis of gold mineral potentials in Anka schist belt northwestern Nigeria using aeromagnetic data interpretation. J Niger Assoc Math Phy. 2019;52:291–8.
13. Danbatta UA, Abubakar IY, Ibrahim AA. Geochemistry of gold deposits in Anka schist belt, northwestern Nigeria. Nigeria J. Chem. Res. 2008;13:19-29.
14. Saibi H, Azizi M, Mogren S. Structural investigations of Afghanistan deduced from remote sensing and potential field data. Acta Geophysics. 2016;64(4):978–1003.
    DOI: 10.1515/acgeo-2016-0046
15. Ge T, Qiu L, He J, Fan Z, Huang X, Xiong S. Aeromagnetic identification and modeling of mafic-ultramafic complexes in the Huangshan-Turaergen Ni-Cu metallogenic belt in NW China: Magmatic and metallogenic implications. Ore Geology Reviews. 2020;127.
    Available:https://doi.org/10.1016/j.oregeorev.2020.103849
16. Olasunkanmi N, Bamigboye O, Saminu O, Salawu N. Interpretation of high- resolution aeromagnetic data of Kaoje and its Environ, western part of the Zuru Schist belt, Nigeria: implication for Fe–Mn occurrence. Heliyon. 2020;6.
    Available:https://doi. org/10.1016/j.heliyon. 2020.e03320 e03320.
17. Aisabokhae J. Geophysical mapping and mineralization characterization of the mesothermal auriferous basement complex in southern Kebbi, NW Nigeria. NRIAG J. Astro. Geophys. 2021; 10(1):443–465.
    Available:https://doi.org/10.1080/ 20909977.2021.2005333
18. Tawey MD, Alhassan DU, Adetona AA, Salako KA, Rafiu AA, Udensi EE. Application of aeromagnetic data to assess the structures and solid mineral potentials in part of north central Nigeria. Journal of

Geography, Environment and Earth Science International. 2020a;24(5):11-29. Article no. JGEESI.58030. ISSN: 2454-7352
DOI: 10.9734/JGEESI/2020/v24i530223

19. Tawey MD, Ibrahim AA, Ehinlaiye AO. Comparative Depth to Magnetic Source Analysis of Shanga (Sheet 96), North-western Nigeria Using Aeromagnetic Data. African Journal of Environmental Sciences and Renewable Energy. 2023a;12(1);56-69.
20. Nwankwoala HO, Ugwu SA, Agada EA. Interpretation of aeromagnetic survey and satellite imagery of jos-plateau, North-Central Nigeria. International Journal of Emerging Engineering Research and Technology. 2017;5(3):1-9.
Available:http://dx.doi.org/10.22259/ijeert.0503001
21. Gaafar I. Integration of geophysical and geological data for delimitation of mineralised zones in Um Naggat area, central eastern desert, Egypt. NRIAG Journal of Astronomy and Geophysics. 2015;4:86-99.
22. Faruwa AR, Qian W, Akinsunmade A, Akingboye AS, Dusabemariya C. Aeromagnetic and remote sensing characterization of structural elements influencing Iron ore deposits and other mineralization in Kabba, Southwestern Nigeria; 2021.
23. Olomo KO, Bayode S, Alagbe SA, Olayanju GM, Olaleye OK. Aeromagnetic mapping and radioelement influence on mineralogical composition of mesothermal gold deposit in part of ilesha schist belt, Southwestern Nigeria. NRIAG Journal of Astronomy and Geophysics. 2022a;11:1:177-192.
DOI: 10.1080/20909977.2022.2057147
24. Eldosouky AM, Elkhateeb SO. Texture analysis of aeromagnetic data for enhancing geologic features using cooccurrence matrices in Elallaqi area, Southeastern Desert of Egyp. NRIAG Journal of Astronomy and Geophysics. 2018;7(2018):155–161.
25. Pendry JB, Holden AJ, Robbins DJ, Stewart WJ. Magnetism from conductors and enhanced nonlinear phenomena. IEEE Trans Microw Theory Tech. 1999;47(11):2075–2084.
DOI: 10.1109/22.798002
26. Akinlalu AA, Adelusi AO, Olayanju GM, Adiat KAN, Omosuyi GO, Anifowose AYB, Akeredolu BE, Aeromagnetic mapping of basement structures and mineralization characterization of Ilesa Schist Belt, Southwestern Nigeria. J. African Earth Sci. 2018;138:383–391.
Available:https://doi.org/10.1016/j.jafrearsci.2017.11.033
27. Uwiduhaye A, Ngaruye JC, Saibi H. Defining potential mineral exploration targets from the interpretation of aeromagnetic data in Western Rwanda. Ore Geol. Rev. 2020;103927.
Available:https://doi.org/10.1016/j.oregeorev.2020.103927
28. Batherham PM, Bullock SJ, Hopgood DN. Tanzania Integrated Interpretation of aeromagnetic and radiometric maps for mineral exploration; 1983.
29. Ojo SB, Edino F, Ako BD, Onuoha KM, Osayande N. Aeromagnetic imaging and characterization of the Anambra basin, Nigeria for magnetic hydrocarbon indicators. Ife Journal of Science. 2012;14(2):207 – 220.
30. Joseph A, Sodiq A, Moses A, Bamidele O. Geological structure and hydrothermal alteration mapping for mineral deposit prospectivity using airborne geomagnetic and multispectral data in Zuru Province, northwestern Nigeria the Egyptian Journal of Remote Sensing and Space Sciences. 2023;26:231-244.
31. Liba AM, Bonde DS, Abbas M, Usman A, Dallhatu B. Geophysical assessment of geologic structures associated with gold mineralization along Garin Hausawa (Izga) using aeromagnetic data. International Journal of Advances in Engineering and Management (IJAEM). 2022;4(2):84-90.
DOI: 10.35629/5252-0402849
32. Kudamnya EA, Andongma WT, Osumeje JO. Hydrothermal mapping of Maru schist belt, north-western Nigeria using remote sensing technique. International Journal of Civil Engineering (IJCE). 2014;3(1):59-66
33. Olomo KO, Bayode S, Alagbe OA, Olayanju GM, Olaleye OK. Multifaceted investigation of porphyry cu-au-mo deposit in hydrothermal alteration zones within the gold field of Ilesha schist belt. Malaysian Journal of Geosciences (MJG). 2022b;6(2):29- 37.
DOI:
http://doi.org/10.26480/mjg.02.2022.29.37
34. Taofeeq OL. Integrated aeromagnetic and aeroradiometric data for delineating lithologies, structures, and hydrothermal

alteration zones in part of southwestern Nigeria. Arabian Journal of Geosciences. 2020;13:775.
Available:https://doi.org/10.1007/s12517-020-05743-7

35. Umaru AO, Kankara AI. Utilizing Landsat-8 sensor operational land image data for hydrothermal alteration mapping within Anka schist belt, northwestern Nigeria. Research Reviews of the Department of Geography, Tourism and Hotel Management. 2020;49-2:127-149
DOI: 10.5937/ZbDght2002127A
36. Umaru AO, Okunlola O, Danbatta UA, Olusegun GO. Lithostructural and hydrothermal alteration mapping for delineation of gold potential zones within Kaiama, Northwestern Nigeria, using airborne magnetic and radiometric data. Arabian Journal of Geosciences. 2022;15:1771.
37. Arogundade AB, Awoyemi MO, Ajama OD, Falade SC, Hammed OS, Dasho OA, Adenik CA. Integrated aeromagnetic and airborne radiometric data for mapping potential areas of mineralisation deposits in parts of zamfara, Northwest Nigeria. Pure and Applied Geophysics; 2021.
Available:https://doi.org/10.1007/s00024-021-02913-w
38. Mohamed, et al. 3-D magnetic inversion and satellite imagery for the Um Salatit gold occurrence, Central Eastern Desert, Egypt. Arabian Journal of Geosciences. 2019;11(21):2018.
DOI: 10.1007/s12517-018-4020-6
39. Nabighian MN. Toward a three-dimensional automatic interpretation of potential field data via generalised Hilbert transforms: Fundamental relations. Geophysics. 1984;49:780–789.
40. Azizi M, Saibi H, Cooper GRJ. Mineral and structural mapping of the Aynak-Logar Valley (Eastern Afghanistan) from hyperspectral remote sensing data and aeromagnetic data. Arabian Journal of Geosciences. 2015;8(12):10911-10918.
DOI: 10.1007/S12517-015-1993-2
41. Gunn PJ. Linear Transformation of Gravity and Magnetic Fields. Geophysical Prospecting. 1975;23:300-312.
Available:http://dx.doi.org/10.1111/j.1365-2478.1975.tb01530.x
42. Cordell L, Grauch VJS. Mapping basement magnetization zones from aeromagnetic data in the San Juan basin, New Mexico. In: Hinze WJ, Ed., the Utility of Regional Gravity and Magnetic Anomaly Maps, Society of Exploration Geophysicists. 1985;181-197.
Available:https://doi.org/10.1190/1.0931830346.ch16
43. Wright JB. Geology and mineral resources of West Africa. George Allen and Unwin, London; 1985.
44. Grant NK. Structural distinction between metasedimentary cover and underlying basement in 600 M.Y. Old Pan-African domain. Geology Society of American Bulletin. 1978;89:50-58.
45. McCurry P. The geology of the precambrian to lower Palaeozoic rocks of Northern Nigeria. A review. In: Kogbe CA (Ed) *Geology of Nigeria*. Lagos: Elizabethan Publishers. 1976;15- 39.
46. Olade MA, Elueze AA. Petrochemistry of the Ilesha amphibolite and Precambrian crustal evolution in the pan-African domain of SW Nigeria. Precambrian Res. 1979;8:303–318.
47. Turner DC. Upper Proterozoic schist belts in the Nigerian sector of the Pan-African Province of West Africa. Precambrian Res. 1983;21:55–79.
48. Ajibade AC, Fitches WR, Wright JB. The Zungeru mylonites, Nigeria: Recognition of a major unit. Rev de Geol Geog Phys. 1979;21:359–363.
49. Truswell JF, Cope RN. The geology of parts of Niger and Zaria Provinces, Northern Nigeria. Geol Suvey Nigeria Bull. 1963;29:1–104.
50. Core D, Buckingham A, Belfield S. Detailed structural analysis of magnetic data done quickly and objectively, SGEG Newsletter; 2009.
51. Kovesi P. Image features from phase congruency, Videre: Journal of Computer Vision Research, Summer. The MIT Press. 1991;1(3):2-27.
52. Kovesi P. Symmetry and asymmetry from local phase, AI '97, Tenth Australian. Joint Conference on Artificial Intelligence. 1997; 2 - 4.
53. Roest WR, Verhoefs J, Pilkington M. Magnetic interpretation using 3-D analytic signal Magnetic interpretation using the 3-D analytic signal. Geophysics. 1992;57(1):116–131.
54. Telford WM, Geldart LP, Sherriff RE, Keys DA. Applied geophysics. Cambridge: Cambridge University Press. 1990;860.
55. Philips JD. Locating magnetic contacts: A comparison of the horizontal gradient,

analytic signal, and local wavenumber methods: Calgary. In: 70th Meeting, society of exploration geophysicists, expanded abstracts with biographies, Technical Program. 2000; 1:402–405.

Peer-review history:
The peer review history for this paper can be accessed here:
https://www.sdiarticle5.com/review-history/115647